*URSI AP-RASC 2019, New Delhi, India, 09 - 15 March 2019*

# Design of Wideband Wearable Antenna using Characteristic Mode Analysis

Sen Yan* (1), and Guy A. E. Vandenbosch(2)
(1) School of Electronics and Information Engineering, Xi'an Jiaotong University, Xi'an, Shaanxi 710049, China
Corresponding E-mail: sen.yan@xjtu.edu.cn
(2) ESAT-TELEMIC Research Div., KU Leuven, Kasteelpark Arenberg 10, Box 2444, 3001 Leuven, Belgium

## Abstract

A wideband wearable antenna for Wireless Body Area Network (WBAN) applications is designed based on characteristic mode analysis (CMA). By using the ground as a part of the radiator, the impedance bandwidth of the antenna is greatly increased. The other performances of the antenna, e.g., the realized gain, radiation efficiency, radiation pattern, and the specific absorption rate (SAR) are analyzed both in free space and on the human body. This wide band behavior provides robustness across different environments and to relatively large fabrication tolerances.

## 1. Introduction

Wearable antennas have attracted more and more attention recently, due to the huge potential in a wide range of applications, e.g. medical monitoring, physical training, care for children and the elderly, emergency rescue services, etc. [1]. However, the design of wearable antennas is a challenge for antenna engineers, since the operating environment of wearable antennas is quite different from the traditional ones [1], [2]. Unavoidable coupling between the antennas and the human bodies, the variable dimensions when wearing on the bodies, and the requirement of thickness, weight and fabrication cost are the several main challenges in the design of wearable antennas.

Several types of wearable antennas have been proposed and studied. A popular one is with the use of conductive textiles [3]-[11], which can be directly integrated with clothes, but textile materials usually have a higher loss than normal conductors and will reduce the total radiation efficiency. Besides, the frequency shift due to the deformations of the flexible materials is a severe problem, especially when considering the inherently narrow bandwidth of microstrip antennas. Another category of wearable antennas are button antennas [12]-[15] ,which can be fabricated from normal conductors and thus own higher radiation efficiencies than the pure textile antennas, but the inherent small size and the low profile of buttons limit their operating bandwidths.

Recently, the chassis antenna has received great attention, linked with the rapid growth of smart mobile terminal development [16]-[18]. The basic idea of the chassis antenna is to use the chassis as a part of the radiator. This way of working is able to efficiently increase the effective aperture of the antenna and the impedance matching bandwidth, especially at lower frequencies. Characteristic mode analysis (CMA) is the main design method to analyze chassis antennas, since it directly yields the basic performance of the chassis without considering the feeding method [16]. Inspired by the chassis antenna as used in mobile terminals, a wearable chassis antenna is proposed in this paper by combining a button and a piece of the textile ground. The simple and robust structure shows a much wider operating band compared to other textile microstrip antennas and button antennas.

## 2. Characteristic Modes of a Textile Sheet

First, the characteristic modes of a 50 mm x 25 mm sheet of conductor is calculated with the commercial solver CST. The first three modes are obtained from 0.5 GHz to 4 GHz and the Modal Significance (MS) is shown in Fig. 1. The dominant mode resonates around 2.65 GHz is characterized by a longitudinal (horizontal) current and is widely used in patch antennas, which also has a good radiation behavior in a wide band above 2.4 GHz. The second mode is characterized by a transversal (vertical) current. The third mode is a special non-resonant mode with a current forming closed loops over the plate [16]. The characteristic current distributions at 2.45 GHz of the first two modes are shown in Fig. 2. This information is crucial in determining the proper location of the feeding structure.

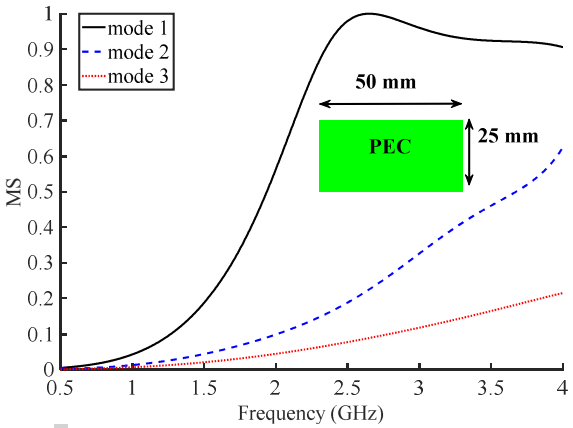


**Figure 1**. Modal Significance (MS) of a connective sheet.

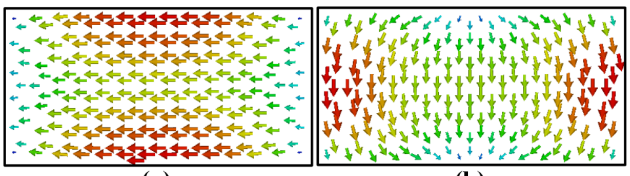


**Figure 2**. Current distributions of the first two modes at 2.45 GHz. (a) the first mode, (b) the second mode.

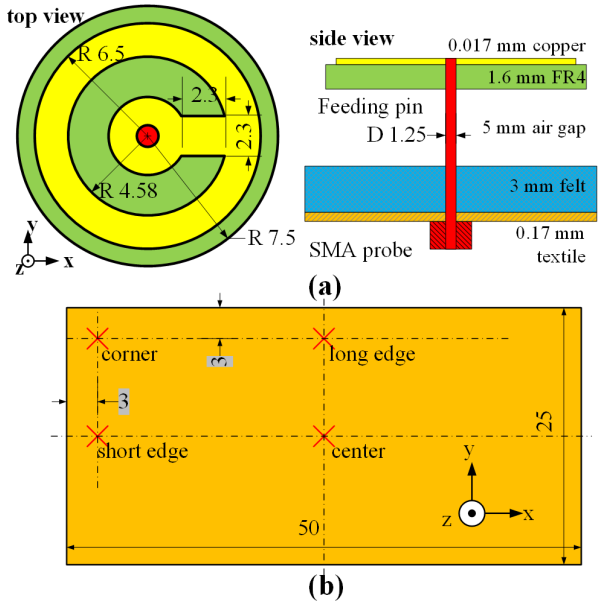


**Figure 3**. Topology (a) and location (b) of the button antenna, dimensions in mm.

## 3. Antenna Design

A button is designed as a top loaded monopole antenna and used to excite the conductive sheet. The detailed dimensions of the proposed monopole are shown in Fig. 3 (a), and four locations on the ground are studies, i.e. the center, the long edge, the short edge, and the corner, see Fig. 4 (b). The antenna is fabricated on a 1.6 mm thick FR4 board ($\varepsilon_r = 4.3$, $\tan\delta = 0.044$) with a diameter of 15 mm. A circular loaded patch with a diameter of 13 mm is printed on the top layer. A complementary split-ring resonator (CSRR) slot is etched within the patch to increase the current path length and thus reduce the size of the button. A 3 mm thick felt ($\varepsilon_r = 1.3$, $\tan\delta = 0.044$) is used to mimic clothes, and the button is located 5 mm higher on the top of the clothes. The ground layer is fabricated with a 0.17 mm thick metallic textile sheet ($\sigma = 1.18 \times 10^5$ S/m), and glued on the bottom of the felt. The button is fed in the center by a standard SMA connector fixed to the textile sheet by metallic glue.

The input impedances and reflection coefficients of all these topologies are given in Fig. 4, and the normalized radiation patterns are revealed in Fig. 5. A configuration with an infinite ground plane (1 m x 1 m ground plane in simulations) is used as a reference. For the reference antenna, the resonant frequency is around 2.18 GHz (the

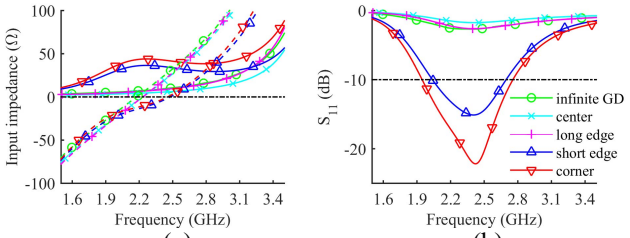


**Figure 4**. Input impedances and reflection coefficients of the button antenna at different locations

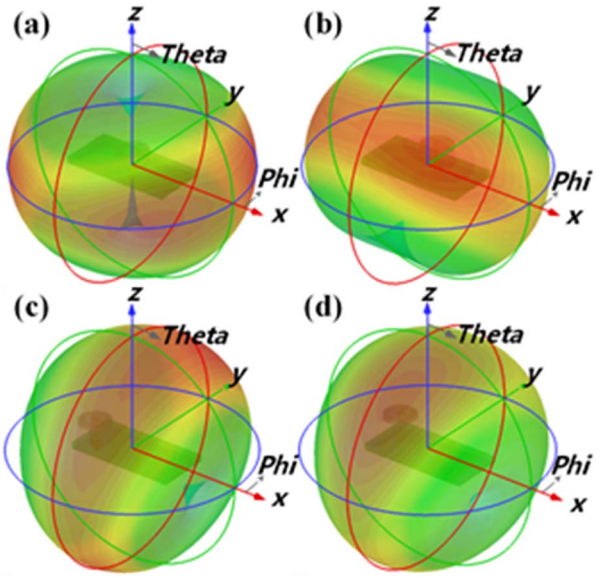


**Figure 5**. Normalized radiation patterns of the button antenna for different locations. (a) center, (b) long edge, (c) short edge, (d) corner.

imaginary part of the input impedance goes through zero), but the real part of the input impedance ($R_{in}$) is only ca. 7 Ω there, which is hard to match to a 50 Ω feeding line and consequently in normal circumstances cannot efficiently radiate. The long edge location will shift the resonant frequency to 2.23 GHz, but the $R_{in}$ nearly does not change. When the button moves to the short edge, its resonance shifts to 2.48 GHz, and the $R_{in}$ increases to ca. 35 Ω. The $R_{in}$ can be even further improved to ca. 40 Ω when the button is located on the corner of the ground. In general, these last two locations are able to provide a quite wide impedance bandwidth, see Fig. 4 (b).

The differences in input impedance for different locations are actually due to the change of the coupling between the button and the textile ground. The most efficient excitation position is the position where the electric field normal to the PEC reaches a maximum (and the current a minimum) [17]. Fig. 2 clearly indicates that the button does not really couple with the first mode of the ground when it is located in the ground center and long edge point, since these are the points with minimum electric field of the first mode. The radiation is mainly due to the button itself, thus its pattern is roughly a monopole-like pattern, which is

omnidirectional in the horizontal plane, see Fig. 5 (a) and (b). The short edge point can obviously couple to the first mode. In this configuration, the textile ground will act as the main radiator of the whole antenna, increasing the real part of the input impedance and the bandwidth (658 MHz around 2.37 GHz). The radiation pattern and the polarization are similar as for a dipole parallel to the x axis, and the realized gain is around 1.8 dBi, see Fig. 5 (c). The corner point couples to both the first and the second mode, further increasing the real part of the input impedance and the matching bandwidth of the antenna (810 MHz around 2.35 GHz).

## 4. Antenna on a Human Body

A mal human model of 175 cm height is used in the calculations, with the complex permittivity of human muscle 52.7+j12.8 at 2.45 GHz. In general, a human shoulder is a desirable location for a button antenna, mainly due to the fact that radiation in horizontal directions from this location is less blocked than for example radiation from an antenna on the chest. To reduce the computational resources needed, only the body above the chest is included in the calculations. The antenna is located on the left shoulder with a 10 mm thick gap to mimic the cloth layer. The angle between the antenna and the horizontal plane is 15°, see Fig. 6.

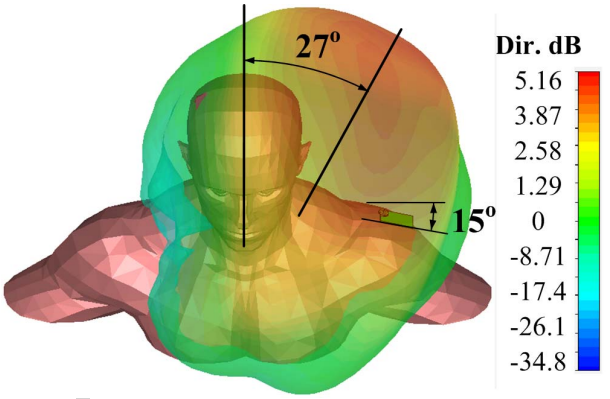


**Figure 6**. Location and radiation pattern of the button in the short edge location.

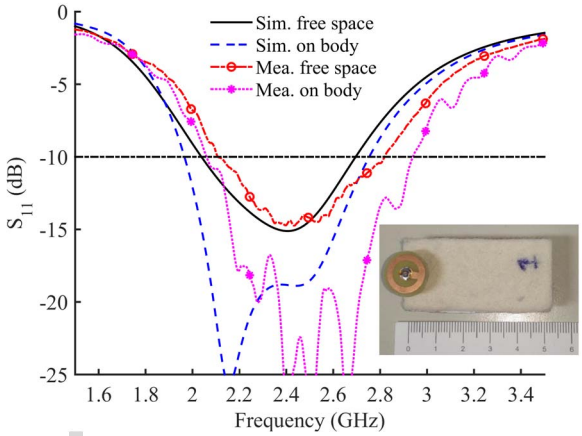


**Figure 7**. Reflection coefficients of the proposed antenna.

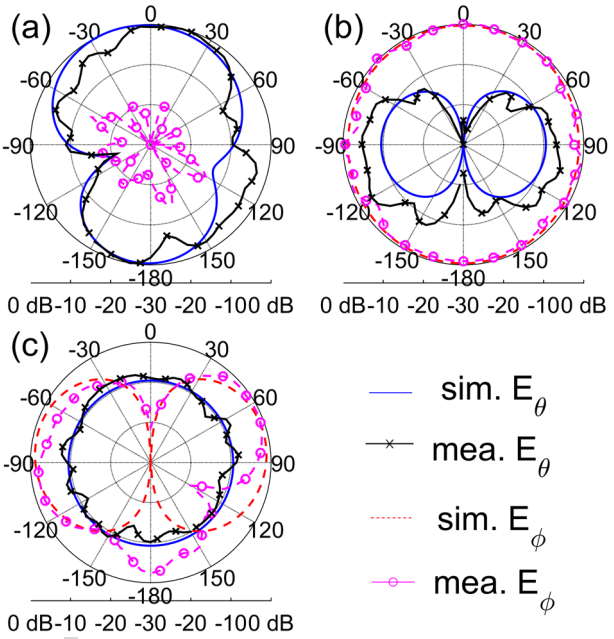


**Figure 8**. Radiation pattern in free space. (a) x-z plane, (b) y-z plane, (c) x-y plane

Although the corner location provides a slightly wider frequency bandwidth, the short edge location is chosen for the fabricated prototype, because its symmetry eases the integration with clothes, and it looks more aesthetic. Our numerical calculation has proved that the corner location has the similar performance compared to the short edge one.

The reflection coefficients of the button antenna in free space and on the human body are compared in Fig. 7. The impedance matching bandwidth of the antenna is quite stable. Actually, the presence of the human body slightly increases the impedance matching bandwidth, due to the relatively high losses of the human tissues. The radiation pattern on human body is shown in Fig. 6. The main beam is 27° away from zenith, and the half power beam widths (HPBW) are 66° and 128° in the XOZ and YOZ planes, respectively. The realized gain of the antenna increases to 5.2 dBi with respect to free space, due to the reflection by the human body. The radiation efficiency is 72.1 %. The relative low value is due to the loss in the human tissue.

A prototype is fabricated and measured to verified our design. The photo and the measured reflection coefficients are shown in Fig. 7. In free space, the measured matching bandwidth shifts up ca. 100 MHz compared to the simulated one. On the shoulder, this shift is 150 MHz. This shift may be attributed to the not-very well defined properties of the textile materials, and to the relatively large tolerances of the manual fabrication process. However, since the matching bandwidth is much wider than the ISM 2.4 GHz band, the antenna shows a very robust performance under all unideal conditions, which is a desirable feature for large scale industrial production.

Fig. 8 reveals the farfiled radiation pattern of the antenna in free space. Measurements agree reasonably well with

simulations, especially in front of the antenna. At the back side the agreement is worse. The reason is that the current in the ground is easily influenced by the feeding connector, ferrite ring, holder, and cables. The measured realized gain is 1.1 dBi at 2.45 GHz, while the simulated realized gain is 1.8 dBi. The measured radiation efficiency is ca. 88 %. More measurement about the farfiled radiation pattern will be arranged in the future.

The SAR values are evaluated based on the IEEE/IEC 62704-1 standard, and the equivalent isotropically radiated power (EIRP) is 20 dBm (input power is 15 dBm). The maximum SAR obtained is ca. 0.18 W/kg, which is much lower than the limitation of 2 W/kg in European.

## 5. Conclusion

A wideband wearable button antenna is designed using the CMA. By analyzing the characteristic modes of the ground, and choosing the suitable location of the button on the ground, a quite robust wide band can be achieved around 2.4 GHz. The antenna is analyzed both in free space and on the human body, and a prototype is fabricated to verify the design.

## 6. Acknowledgements

This work was partly supported by the Research Founation-Flanders (F.W.O.) Postdoctoral Fellowship (No. 2O1217N)

## 7. References

1. P. S. Hall, and Y. Hao, “Antennas and Propagation for Body-Centric Wireless Communications (2nd Edition),” Artech House, 2012.

2. S. Yan, P. J. Soh, and G. A. E. Vandenbosch, “Made to be Worn,” Elect. Lett., **50**, 6, Mar. 2014, pp. 420.

3. H. Wang, Z. Zhang, Y. Li, and Z. Feng, “A Dual Resonant Shorted Patch Antenna for Wearable Application in 430 MHz Band,” IEEE Trans. Antennas Propag., **61**, 12, Dec. 2013, pp. 6195-6200.

4. S. Agneessens, and H. Rogier, “Compact Half Diamond Dual-Band Textile HMSIW On-Body Antenna,” IEEE Trans. Antennas Propag., **62**, 5, May 2014, pp. 2374-2381.
5. S. Yan, P. J. Soh, and G. A. E. Vandenbosch, “Compact all-textile dual-band antenna loaded with metamaterial inspired structure,” IEEE Antennas Wireless Propag. Lett., **14**, 2015, pp. 1486-1489.

6. S. Yan, P.J. Soh, and G.A.E. Vandenbosch, “Dual-Band Textile MIMO Antenna Based on Substrate Integrated Waveguide (SIW) Technology,” IEEE Trans. Antennas Propag., **63**, 11, Nov. 2015, pp. 4640-4647.

7. S. Zhu, and R. Langley, “Dual-band wearable textile antenna on an EBG substrate,” IEEE Trans. Antennas Propag., **57**, 4, Apr. 2009, pp. 926-935.

8. Z. H. Jiang, E. B. Donovan, E. S. Peter, and H. W. Douglas, “A compact, low-profile metasurface-enabled antenna for wearable medical body-area network devices,” IEEE Trans. Antennas Propag., **62**, 8, 2014, pp. 4021-4030.
9. S. Yan, P. J. Soh, and G. A. E. Vandenbosch, “Low-profile dual-band textile antenna with artificial magnetic conductor plane,” IEEE Trans. Antennas Propag., **62**, 12, Dec. 2014, pp. 6487-6490.

10. S. Yan, P. J. Soh, and G.A.E. Vandenbosch, “Wearable Dual-Band Magneto-Electric Dipole Antenna for WBAN/WLAN Applications,” IEEE Trans. Antennas Propag., **63**, 9, Sep. 2015, pp. 4165-4169.

11. S. Yan, V. Volskiy and G. A. E. Vandenbosch, "Compact Dual-Band Textile PIFA for 433-MHz/2.4-GHz ISM Bands,” Antennas Wireless Propag. Lett., **16**, 2017, pp. 2436-2439.

12. B. Mandal and S. K. Parui, “A Miniaturized Wearable Button Antenna for WLAN and Wi-Max Application using Transparent Acrylic Sheet as Substrate,” Microwave. Opt. Technol. Lett., **57**, 1, Jan. 2015, pp. 45-49.

13. B. Sanz-Izquierdo, J. C. Batchelor and M. I. Sobhy “Button Antenna on Textiles for Wireless Local Area Network on Body Applications,” IET Microw. Antennas Propag, **4**, 11, Nol. 2010, pp. 1980–1987.

14. X. Y. Zhang, H. Wong, T. Mo and Y. F. Cao, "Dual-Band Dual-Mode Button Antenna for On-Body and Off-Body Communications," IEEE Trans. Biomed. Circuits Syst., **11**, 4, Aug. 2017, pp. 933-941.

15. H. Xiaomu, S. Yan, G. A. E. Vandenbosch, "Wearable Button Antenna for Dual-Band WLAN Applications With Combined on and off-Body Radiation Patterns," IEEE Trans. Antennas Propag., **65**, 3, Mar. 2017, pp. 1384-1387.

16. M. Cabedo-Fabres, E. Antonino-Daviu, A. Valero-Nogueira, and M. F. Bataller, “The theory of characteristic modes revisited: A contribution to the design of antennas for modern applications,” IEEE Antennas Propag. Mag., **49**, 5, Oct. 2007, pp. 52-68.

17. H. Li, Y. Tan, B. K. Lau, Z. Ying, and S. He, “Characteristic mode based tradeoff analysis of antenna-chassis interactions for multiple antenna terminals,” IEEE Trans. Antennas Propag., **60**, 2, Feb. 2012, pp. 490-502.

18. N. L. Bohannon, and J. T. Bernhard, “Design Guidelines Using Characteristic Mode Theory for Improving the Bandwidth of PIFAs,” IEEE Trans. Antennas Propag., 63, 2, Feb. 2015, pp. 459-465.